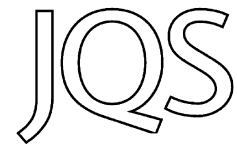


The influence of ice marginal setting on early Holocene retreat rates in central West Greenland



SAMUEL E. KELLEY,^{1,2*} JASON P. BRINER¹ and SUSAN R. H. ZIMMERMAN³

¹Geology Department, University at Buffalo, NY, USA

²Earth and Environmental Sciences, University of Waterloo, 200 University Ave. W, Waterloo, Ontario, Canada N2L 3G1

³Center for AMS, Lawrence Livermore National Laboratory, CA, USA

Received 3 December 2014; Revised 25 February 2015; Accepted 9 March 2015

ABSTRACT: Ice sheet reconstructions from diverse ice margin settings, spanning multiple millennia, are needed to assess the reaction of the Greenland Ice Sheet (GrIS) to millennial-scale climatic forcing and to place historical records in a longer-term context. Here we present 18 new cosmogenic ¹⁰Be exposure ages and five new radiocarbon ages that constrain the early Holocene retreat of the GrIS in the Disko Bugt region in both a marine and a land-based setting. Results indicate similar rates of early Holocene retreat of ~40–50 m a⁻¹ from transects in Torsukattak fjord (marine setting) and the Naternaq area (land-based setting). We compile seven previously published chronologies of deglaciation from West Greenland, which yield early Holocene retreat rates ranging from 10 to 65 m a⁻¹, similar to those determined for our two study areas. This work demonstrates that when averaged on millennial timescales, retreat rates were remarkably similar along the western GrIS margin. Furthermore, the retreat rates calculated here demonstrate that terrestrial sectors of ice sheets can retreat at net rates comparable to their marine counterparts. Copyright © 2015 John Wiley & Sons, Ltd.

KEYWORDS: ¹⁰Be exposure dating; Greenland Ice Sheet; Holocene.

Introduction

Scrutiny of recent Greenland Ice Sheet (GrIS) change has provided valuable insight into its response to past and ongoing climate change (e.g. Zwally *et al.*, 2002; Holland *et al.*, 2008; Khan *et al.*, 2014). The historical record reveals a complex picture of GrIS behavior over the past two centuries (Weidick, 1968, 1994; Bjørk *et al.*, 2012; Kjær *et al.*, 2012). This complex picture highlights the significant variability exhibited in ice margin change along the periphery of the GrIS (Moon and Joughin, 2008; Bjørk *et al.*, 2012). For example, marine-terminating glaciers in West Greenland have retreated an order of magnitude more than land-terminating glaciers during the 19th–21st centuries, probably due to differences in their sensitivity to climate forcing (Weidick, 1994; Kelley *et al.*, 2012). However, it is challenging to identify the influence of climate change on ice margin change in the brief observational record, due to influential ice sheet dynamics in some sectors. Reconstructions of ice margin fluctuations spanning the Holocene can be used to provide a longer term perspective on the response of the GrIS to a warming climate.

Our knowledge of fluctuations of the GrIS during the Holocene has expanded in recent years (Möller *et al.*, 2010; Long *et al.*, 2011; Levy *et al.*, 2012; Briner *et al.*, 2014; Dyke *et al.*, 2014). This is especially true along the western GrIS margin where new chronologies provide detailed snapshots of Holocene ice margin fluctuations (e.g. Young *et al.*, 2011a; Young *et al.*, 2013a; Levy *et al.*, 2012; Kelley *et al.*, 2013), as well as studies that track movement of the ice margin over many millennia (Weidick and Bennike, 2007; Weidick *et al.*, 2012; Cofaigh *et al.*, 2013; Roberts *et al.*, 2013; Lane *et al.*, 2014; Larsen *et al.*, 2014). Despite these records advancing our knowledge of past GrIS ice margin changes, they are dominated by marine-terminating outlet glaciers, and have not focused on how ice margins behave in varying settings during changes in climate.

Here, we constrain the timing and rate of early Holocene retreat in two contrasting glacial systems in West Greenland –

one marine-based and one land-based system – using 18 new ¹⁰Be ages and five new radiocarbon ages. We use our new chronology to compare the behavior of marine- and land-based glacier systems during early Holocene warming. This comparison allows us to evaluate similarities and differences in the retreat of these early Holocene glacier systems in the context of modern observations of GrIS outlet glacier behavior.

Setting

The Disko Bugt region

We selected two paleo-glacier systems in the Disko Bugt region, central West Greenland, to build chronologies detailing early Holocene retreat. The Torsukattak fjord (northern Disko Bugt) and Nordenskiöld Gletscher (southern Disko Bugt) study areas present two contrasting paleo-glacier systems, one marine-based and one land-based (Fig. 1). We reconstruct the timing and rate of retreat at each site in response to early Holocene warming (~11.7–8.2 ka), estimated from ice cores to be ~6 °C in central Greenland (Vinther *et al.*, 2009). The two study areas presently experience similar climatic conditions (Box, 2002), and are separated by a distance of ~175 km.

Torsukattak fjord is located in northernmost Disko Bugt, south of the peninsula of Nuussuaq (Figs 1 and 2A). The GrIS presently drains into the fjord via Sermeq Kujalleq and Sermeq Avannarleq, major outlet glaciers separated by a nunatak. The region is characterized by high relief, with water depths exceeding 500 m (Rignot *et al.*, 2010), and fjord walls that rise to >600 m above sea level (asl). The fjord connects to Baffin Bay via Disko Bugt to the south-west and through the Vaigat Strait to the north-west. At present, oceanographic circulation at the mouth of Torsukattak fjord is influenced by a limb of the warm West Greenland Current (WGC), which flows from the south-west through Disko Bugt, exiting through Vaigat Strait (Seidenkrantz *et al.*, 2008). Warm water from the WGC penetrates into Torsukattak fjord, causing basal melting along glacier margins at the fjord head (Rignot *et al.*, 2010).

*Correspondence: Samuel E. Kelley, ²Earth and Environmental Sciences, as above. E-mail: samuel.kelley@uwaterloo.ca

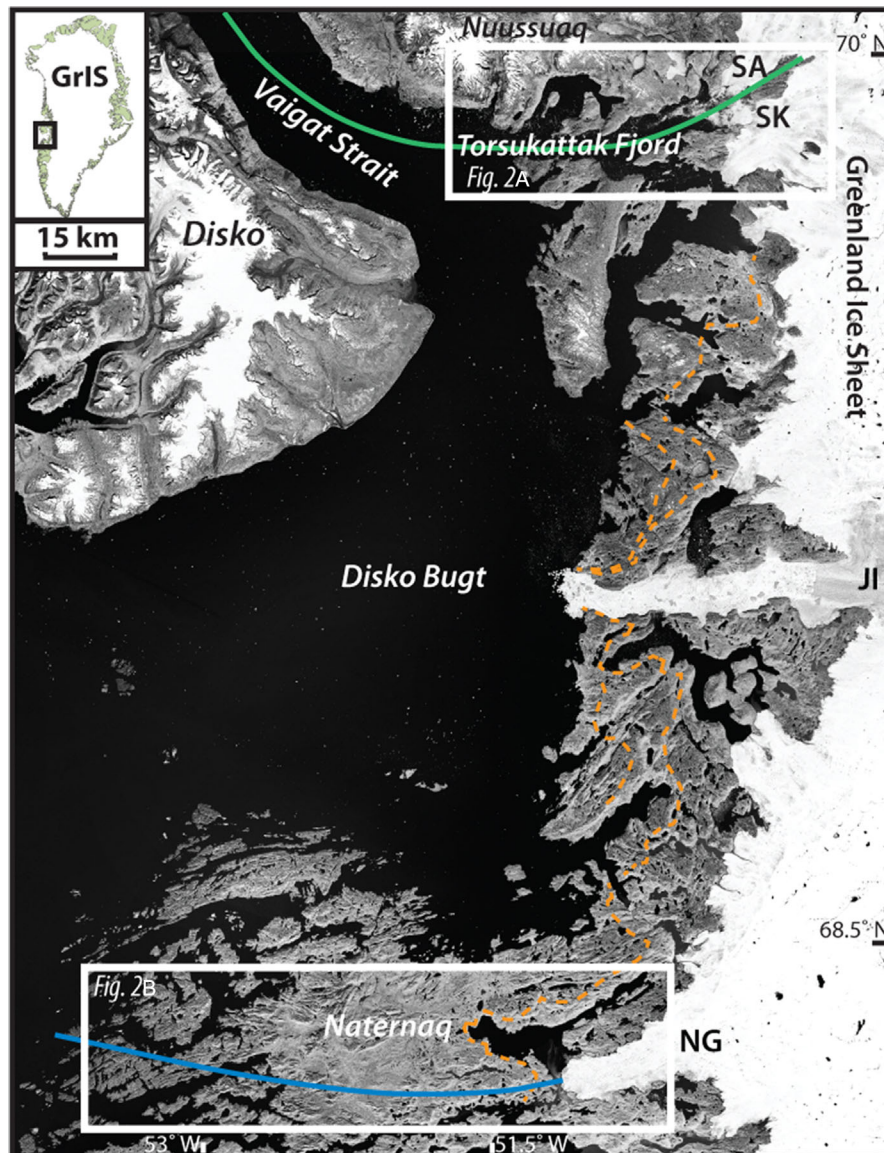


Figure 1. The Disko Bugt region showing the location of the two study areas (white boxes): SA, Sermeq Avannarleq; SK, Sermeq Kujalleq; JI, Jakobshavn Isbræ; NG, Nordenskiöld Gletscher. Solid lines denote transect locations used in Fig. 4 and the orange dotted line marks the Fjord Stade Moraines. Inset map shows the location of Disko Bugt (black box) in Greenland. (For interpretation of the references to color in this figure legend, the reader is referred to the online version of this article.) This figure is available in colour online at wileyonlinelibrary.com.

The Naternaq study area is located along the 90-km-wide ice-free corridor that separates Baffin Bay from the GrIS margin at Nordenskiöld Gletscher (Fig. 1). The Naternaq area is characterized by rounded bedrock hills reaching ~450 m asl. Low-lying areas are filled with glaciomarine sediments and till (Weidick, 1974). Limited ice flow indicators suggest that flow was roughly east-to-west across the region, with a possible change in flow occurring late during deglaciation, routing ice along a more north-easterly flowline into Disko Bugt (Weidick, 1974). A belt of north-south-trending moraines crosses the field area about 5 km west and 10 km north of Nordenskiöld Gletscher (Fig. 2B), and has been mapped as part of the Fjord Stade Moraine belt (Weidick, 1968).

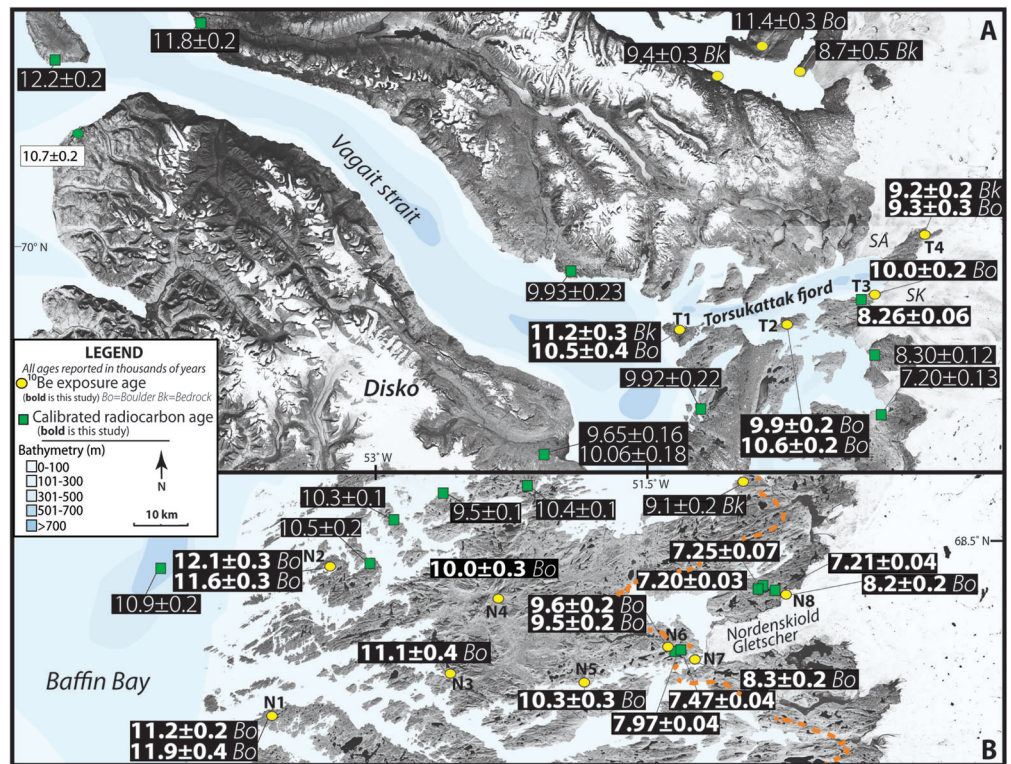
Glacial history

Torsukattak fjord

South-west of the study area, the deglaciation of the Disko Bugt region of West Greenland initiated on the continental shelf by $13\,900 \pm 100$ cal a BP, perhaps reaching as far east as Disko Island by 12.2 ± 0.6 ka [Rinterknecht *et al.*, 2014; all cosmogenic-nuclide exposure ages are calculated using the Arctic production rate (Young *et al.*, 2013b) with the Lal/Stone scaling scheme (Lal, 1991; Stone, 2000); all radiocarbon ages are presented in calibrated years as the mean \pm half

of the one-sigma age range; ages are calibrated using Calib version 7.0 (calib.qub.ac.uk/), with marine ages using the MarineCal13 and a ΔR of 140 ± 25 based on Lloyd *et al.* (2011) and terrestrial ages using the IntCal13 dataset], with a brief readvance at $12\,000 \pm 200$ cal a BP (Ó Cofaigh *et al.*, 2013). Radiocarbon and ^{10}Be ages from the mouth of Disko Bugt place deglaciation at between 11 and 10 ka ($n=16$; Donner and Jungner, 1975; Frich and Ingólfsson, 1990; Ingólfsson *et al.*, 1990; Long and Roberts, 2002; Long *et al.*, 2003; Long *et al.*, 2011; Kelley *et al.*, 2013), with a radiocarbon date on foraminifera from a marine sediment core collected in inner Disko Bugt suggesting the area was ice-free by $10\,200 \pm 100$ cal a BP (Lloyd *et al.*, 2005). Limited radiocarbon dating constrains eastward retreat of the GrIS in the Torsukattak fjord study area (Fig. 2A). A radiocarbon age from a bulk gyttja sample constrains deglaciation before 9920 ± 220 cal a BP south of the fjord mouth; a second radiocarbon age of 9930 ± 230 cal a BP from marine shells constrains deglaciation west of the fjord mouth (Tauber, 1960; Weidick, 1968; Long *et al.*, 1999). Similar ages from eastern Disko place minimum constraints on deglaciation at $10\,060 \pm 180$ and 9650 ± 160 cal a BP based on bulk gyttja and shells, respectively (Ingólfsson *et al.*, 1990). Weidick and Bennike (2007) infer that the Marrait moraine, dated elsewhere in Disko Bugt to 9.2 ka (Young *et al.*, 2011b),

Figure 2. (A) The Torsukattak (top), and (B) Naternaq (bottom) study areas showing the location of ^{10}Be (yellow circles) and radiocarbon ages (green squares) in thousands of years; ages in bold are from this study; ages in plain font are from previous work mentioned in the text. Bathymetric data are from Hogan *et al.* (2012). Orange dotted line in panel B marks the position of the Fjord Stade Moraines. SA, Sermeq Avannarleq; SK, Sermeq Kujalleq. (For interpretation of the references to color in this figure legend, the reader is referred to the online version of this article.) This figure is available in colour online at wileyonlinelibrary.com.



intersects the mouth of Torsukattak fjord. This may be corroborated by a marine geophysical study that suggests the ice margin may have paused there during retreat at ~ 9.9 ka, followed by continuous recession up the fjord (Hogan *et al.*, 2012). Radiocarbon ages related to deglaciation from the inner fjords of northern Disko Bugt are sparse, with a single minimum constraint on deglaciation, ~ 15 km south of Torsukattak fjord, that places local deglaciation before 8300 ± 120 cal a BP (Ingólfsson *et al.*, 1990).

Naternaq

Chronology pertaining to the early Holocene deglaciation of the Naternaq study area comes primarily from north and west of the field area (Fig. 2B). A minimum-limiting radiocarbon age from a bivalve collected in a marine sediment core in nearshore Baffin Bay, north-west of the study area, is $10\,900 \pm 200$ cal a BP (Quillmann *et al.*, 2009; Jennings *et al.*, 2014). Radiocarbon ages from the southern margin of Disko Bugt suggest deglaciation between 11 and 10 ka. For example, a basal date from bulk sediment collected in a lake sediment core places deglaciation in south-westernmost Disko Bugt before $10\,500 \pm 200$ cal a BP (Long and Roberts, 2002). Additional radiocarbon ages from bulk sediment in lake sediment cores collected farther east along the southern margin of Disko Bugt are $10\,400 \pm 100$ cal a BP (Long *et al.*, 2003) and $10\,300 \pm 100$ cal a BP (Long and Roberts, 2002) and an age of 9500 ± 200 cal a BP on shells collected from a raised marine deposit (Donner and Jungner, 1975). ^{10}Be ages from south-western Disko Bugt are slightly older than the radiocarbon ages. A 5-km-long transect of ages, which decreases in age to the south, places retreat of ice out of Disko Bugt by 11.0 ± 0.2 ka at the northern point in the transect, 10.9 ± 0.2 ka at the middle of the transect and an average age of 10.4 ± 0.2 ka ($n=2$) at the southern end (Kelley *et al.*, 2013). Closer to the present ice margin, ~ 30 km north of Nordenskiöld Gletscher, a radiocarbon age from a bulk sediment sample (9600 ± 200 cal a BP) and ^{10}Be ages

(9.2 ± 0.1 ka; $n=2$) are in good agreement on the timing of ice retreat onto the mainland (Long and Roberts, 2002; Young *et al.*, 2013a). Surficial mapping places the Fjord Stade moraines roughly parallel to, and 5–10 km beyond, the right-lateral and terminal margins of Nordenskiöld Gletscher (Weidick, 1968), indicating that the ice margin resided in that area between 9.3 and 8.2 ka (Young *et al.*, 2013a). Finally, ^{10}Be ages from adjacent to the present ice margin ~ 55 km to the north of Nordenskiöld Gletscher, suggest ice retreated behind the present ice margin by 7.0 ± 0.1 ka (Kelley *et al.*, 2012).

Methods

We collected samples for ^{10}Be dating along two transects roughly perpendicular to the present ice margin, with one transect located along the southern margin of Torsukattak fjord and the second in the Naternaq region. We collected lake sediment cores from four lakes in the Naternaq study area to obtain basal radiocarbon dating constraints on deglaciation (see supporting Fig. S1; Fig. 2). Full details of ^{10}Be and radiocarbon dating methods are given in the supporting information (Appendix S1).

Results

^{10}Be dating

Torsukattak fjord

Seven samples for ^{10}Be dating were collected from four locations on a west–east transect along the southern margin of Torsukattak fjord (Fig. 2A; Table 1). Two ^{10}Be ages from outer Torsukattak fjord (site T1) derived from bedrock and a boulder yield ages of 11.2 ± 0.3 and 10.5 ± 0.4 ka, respectively, and average 10.9 ± 0.5 ka (all averages are mean \pm one SD). Two boulders from a mid-fjord location (site T2) yield ^{10}Be ages of 10.6 ± 0.2 and 9.9 ± 0.2 ka, which average 10.3 ± 0.5 ka. A ^{10}Be age from about 2 km west of Sermeq

Table 1. Sample information for ^{10}Be ages.

Sample name	Latitude (°N)	Longitude (°W)	Elevation (m)	Sample type	Thickness (cm)	Shielding correction	Quartz (g)	^9Be (μg)	$^{10}\text{Be}/^9\text{Be} \pm 1\sigma$ (10^{-13})	^{10}Be (atoms g^{-1})	^{10}Be uncertainty (atoms g^{-1})	^{10}Be age $\pm 1\sigma$ (ka)
Torsukattak fjord												
12GRO-02	70.0952	50.0276	507	Boulder	1.0	1.0	27.919	227.67	1.208 ± 0.040	$6.58\text{E}+04$	$2.20\text{E}+03$	9.3 ± 0.3
12GRO-04	70.0959	50.0315	499	Bedrock	2.0	1.0	60.020	265.07	2.377 ± 0.045	$7.02\text{E}+04$	$1.32\text{E}+03$	9.2 ± 0.2
12GRO-20	69.9119	51.4045	261	Boulder	2.0	1.0	39.493	225.81	1.521 ± 0.055	$5.81\text{E}+04$	$2.10\text{E}+03$	10.5 ± 0.4
12GRO-22	69.9119	51.4053	271	Bedrock	1.0	1.0	50.160	226.11	2.094 ± 0.061	$6.31\text{E}+04$	$1.83\text{E}+03$	11.2 ± 0.3
12GRO-23	69.9209	50.8022	360	Boulder	2.0	1.0	47.774	225.59	2.060 ± 0.046	$6.50\text{E}+04$	$1.46\text{E}+03$	10.6 ± 0.2
12GRO-24	69.9208	50.8018	352	Boulder	2.0	1.0	51.395	226.11	2.053 ± 0.051	$6.03\text{E}+04$	$1.51\text{E}+03$	9.9 ± 0.2
12GRO-34	69.9783	50.3179	102	Boulder	2.0	1.0	38.003	226.07	1.177 ± 0.027	$4.68\text{E}+04$	$1.06\text{E}+03$	10.0 ± 0.2
Naternaq												
13GRO-04	68.4115	50.8187	240	Boulder	2.0	1.0	27.733	226.48	0.818 ± 0.022	$4.46\text{E}+04$	$1.22\text{E}+03$	8.2 ± 0.2
13GRO-10	68.2454	51.8504	316	Boulder	2.0	1.0	37.460	226.37	1.500 ± 0.039	$6.60\text{E}+04$	$1.59\text{E}+03$	10.3 ± 0.3
13GRO-13	68.2588	52.4822	234	Boulder	2.0	1.0	30.496	226.00	1.222 ± 0.046	$60.5\text{E}+04$	$2.28\text{E}+03$	11.1 ± 0.4
13GRO-16	68.1689	53.3892	231	Boulder	2.0	1.0	35.644	226.33	1.435 ± 0.030	$6.09\text{E}+04$	$1.27\text{E}+03$	11.2 ± 0.2
13GRO-17	68.1685	53.3883	224	Boulder	2.0	1.0	30.513	227.56	1.287 ± 0.039	$6.41\text{E}+04$	$1.94\text{E}+03$	11.9 ± 0.4
13GRO-20	68.4493	53.1182	143	Boulder	3.0	1.0	39.041	227.34	1.518 ± 0.039	$5.91\text{E}+04$	$1.52\text{E}+03$	12.1 ± 0.3
13GRO-21	68.4493	53.1182	144	Boulder	2.0	1.0	31.365	225.70	1.188 ± 0.035	$5.71\text{E}+04$	$1.67\text{E}+03$	11.6 ± 0.4
13GRO-26	68.3990	52.2744	209	Boulder	2.0	1.0	27.900	226.52	0.972 ± 0.030	$5.27\text{E}+04$	$1.65\text{E}+03$	10.0 ± 0.3
13GRO-28	68.2874	51.2841	77	Boulder	1.0	1.0	32.812	225.55	0.835 ± 0.017	$3.83\text{E}+04$	$7.83\text{E}+02$	8.3 ± 0.2
13GRO-34	68.3165	51.3800	271	Boulder	1.0	1.0	30.745	225.10	1.110 ± 0.026	$5.43\text{E}+04$	$1.29\text{E}+03$	9.6 ± 0.2
13GRO-35	68.3165	51.3823	266	Boulder	1.0	1.0	32.632	222.57	1.183 ± 0.022	$5.93\text{E}+04$	$1.02\text{E}+03$	9.5 ± 0.2

All samples were spiked with a $372.5 \mu\text{g g}^{-1}$ ^9Be carrier; AMS results are standardized to 07KNSTD; ratios are blank-corrected, and shown at 1-sigma uncertainty.

Kujalleq (site T3) derived from bedrock yields an age of 10.0 ± 0.2 ka. One bedrock sample and one boulder sample collected from the nunatak at the head of Torsukattak fjord (site T4) yield ages of 9.2 ± 0.2 and 9.3 ± 0.3 ka, respectively, and average 9.3 ± 0.1 ka.

Naternaq

Eleven boulder samples were collected from bedrock hills above local marine limit along a west–east transect from Baffin Bay to Nordenskiöld Gletscher (Fig. 2B; Table 1). Two samples collected from a hilltop on the Baffin Bay coastline (site N1) yield ages of 11.2 ± 0.2 and 11.9 ± 0.4 ka and average 11.6 ± 0.5 ka. To the south, two samples collected at site N2, also on the Baffin Bay coastline, yield ages of 12.1 ± 0.3 and 11.6 ± 0.3 ka and average 11.9 ± 0.4 ka. About 50 km east of the coast, a single boulder from site N3 yields an age of 11.1 ± 0.4 ka. In central Naternaq a perched erratic boulder on a bedrock hilltop, site N4, yields an age of 10.0 ± 0.3 ka. On the southern margin of the study area, ~ 100 km east of the coast and ~ 30 km west of the Nordenskiöld Gletscher terminus, an erratic at site N5 yields an age of 10.3 ± 0.3 ka. Two boulder samples collected at site N6, >1 km outboard of a flight of moraines mapped as the Fjord Stade Moraines and located about 5 km west of Nordenskiöld Gletscher, yield ages of 9.6 ± 0.2 and 9.5 ± 0.2 ka and average 9.5 ± 0.1 ka (Fig. 3). A boulder sample collected at site N7, ~ 4 km inboard of the moraines and ~ 4 km west of the Nordenskiöld Gletscher terminus, yields an age of 8.3 ± 0.2 ka. The easternmost sample in our transect, collected ~ 0.5 km from the present Nordenskiöld Gletscher margin (site N8) and inboard of the Fjord Stade Moraines, yields an age of 8.2 ± 0.2 ka.

Radiocarbon

Torsukattak fjord

In Torsukattak fjord, raised marine deposits reach an elevation of ~ 30 m asl. A radiocarbon age of 8260 ± 60 cal a BP was obtained from paired mollusk valves (*Hiattella arctica*) in

growth position collected from a raised marine deposit (15 m asl), about 5 km west of the Sermeq Kujalleq calving margin (Fig. 2A; Table 2). Although the shell has an unknown relationship to the marine limit, its age nonetheless places a minimum constraint on the deglaciation of the inner fjord.

Naternaq

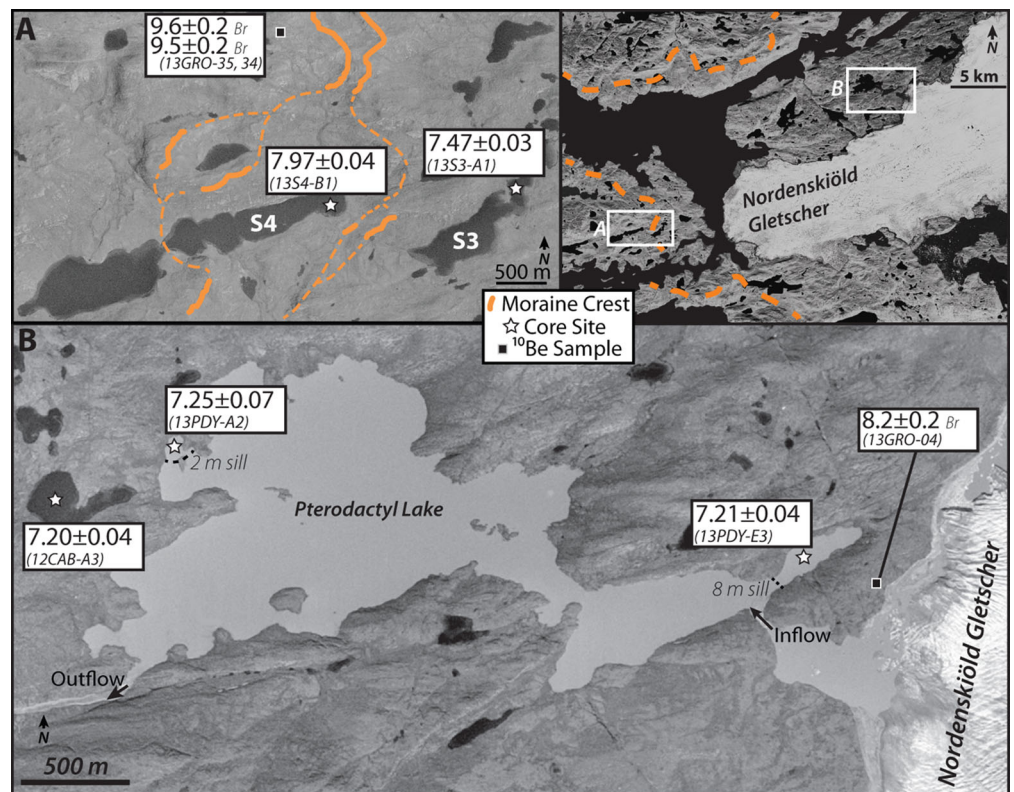
We obtained five basal radiocarbon ages from four lakes from the Naternaq study area that provide minimum limiting constraints on deglaciation (Figs 2B and 3A; Table 2; for core descriptions see Appendix S2 and Fig. S1). Basal sediments from two isolation basins (informal names S3 and S4) located 5.5 km west of Nordenskiöld Gletscher and within the Fjord Stade Moraines (Fig. 3) yielded ages of 7970 ± 40 cal a BP (a marine bivalve fragment from S4) and 7470 ± 40 cal a BP (macrofossils from S3). Two lakes (one proglacial and one non-glacial) near the right-lateral flank of Nordenskiöld Gletscher were also cored (Fig. 3B). Cores from two basins in Pterodactyl Lake (proglacial) yielded ages from macrofossils of 7210 ± 40 and 7250 ± 70 cal a BP. A single core from a nearby Cab Lake (non-glacial) yielded a radiocarbon age on macrofossils of 7200 ± 30 cal a BP.

Discussion

Late Pleistocene deglaciation in west Greenland

The 18 ^{10}Be ages and five radiocarbon ages presented here provide constraints on the deglaciation of the GrIS in both marine- and land-based ice marginal settings (Figs 2 and 4). Our ^{10}Be ages from outer Torsukattak fjord (site T1) place ice retreat from Vaigat Strait and into Torsukattak fjord by 10.9 ± 0.5 ka, and are ~ 1000 years older than previously published minimum limiting radiocarbon ages on deglaciation from the area (Fig. 2A; Tauber, 1960; Weidick, 1968; Long *et al.*, 1999). The ^{10}Be ages demarcate the eastward retreat of the GrIS up Torsukattak fjord, indicating that the mid-fjord deglaciated at 10.3 ± 0.5 ka (site T2), and that the fjord head became ice-free at 10.0 ± 0.2 ka (site T3). Thinning

Figure 3. Aerial photographs taken in 1985 showing lakes S3 and S4 (A) and Pterodactyl and Cab lakes (B), with coring locations (stars), ^{10}Be sample locations and the position of the Fjord Stade Moraines (crests as orange lines). Ice flow in the image was east to west. Inset in the upper right is a Landsat image showing the locations of A and B of the enlarged area with reference to Nordenskiöld Gletscher. (For interpretation of the references to color in this figure legend, the reader is referred to the online version of this article.) This figure is available in colour online at wileyonlinelibrary.com.



and retreat of the ice margin exposed a nunatak ~10 km north-east of the present fjord head at 9.3 ± 0.1 ka (site T4). Our minimum-limiting radiocarbon age from the fjord head of 8260 ± 60 cal a BP is consistent with our ^{10}Be chronology.

Our ^{10}Be ages from the westernmost sites in the Natanaq study area, sites N1 and N2, constrain GrIS retreat onto land at 11.7 ± 0.3 ka ($n=4$; Fig. 2B). The GrIS continued eastward retreat, reaching site N3 at 11.1 ± 0.4 ka, N4 at 10.0 ± 0.3 ka and N5 at 10.3 ± 0.3 ka. Deglaciation continued eastward, with ages of 9.6 ± 0.1 ka at site N6, outboard of the Fjord Stade Moraines, and 8.3 ± 0.2 ka (site N7) inboard of the moraines. These ages are supported by minimum-limiting radiocarbon ages from lakes S3 and S4 of 7470 ± 40 and 7970 ± 40 cal a BP, respectively (Figs 2B and 3A).

The easternmost ^{10}Be age in the study area of 8.2 ± 0.2 ka was obtained from site N8, ~250 m north of the right-lateral flank of Nordenskiöld Gletscher, with two radiocarbon ages from a proglacial threshold lake, Pterodactyl Lake, placing the retreat of the GrIS from the lake's catchment at 7230 ± 30 cal a BP ($n=2$). The difference between the ^{10}Be age from near the ice margin and radiocarbon ages from within Pterodactyl Lake allows a number of possible scenarios: (1) these ages indicate that GrIS meltwater drained into the Pterodactyl Lake catchment for as long as 1000 years after it retreated from site N8; (2) a significant lag exists between deglaciation registered by ^{10}Be ages and a change in sedimentation in the lakes due to local stagnant ice or unstable hill slopes; (3) there is significant error in one or all the ages. We feel that scenario 1 is unlikely given similarity in basal ages from the small-catchment Cab Lake and proglacial Pterodactyl Lake. Scenario 2 is plausible, as it is logical that some lag exists between a glacier exiting a catchment and a change from minerogenic to organic sedimentation. That said, a study from the Jakobshavn area documents a short-lived (decadal scale) advance and retreat of the GrIS in and out of a lake's catchment (Young *et al.*,

2011b), suggesting that a lag in change of sedimentation of ~1000 years may be unlikely. Scenario 3 cannot be proven or disproven given the present information, although the radiocarbon ages from Nordenskiöld Gletscher are internally consistent ($n=3$), and the ^{10}Be age is from a single sample.

Fjord stade moraines

The Fjord Stade Moraines form a prominent moraine belt that spans central West Greenland (Weidick, 1968; Funder *et al.*, 2011). In the Disko Bugt region, the Fjord Stade Moraines have been precisely dated to correlate with the 9.3- and 8.2-ka cold events (Young *et al.*, 2011a). The ^{10}Be ages from sites N6 and N7 bracket the deposition of the moraine between 9.6 ± 0.1 and 8.3 ± 0.2 ka, confirming the earlier interpretation that they are part of the Fjord Stade Moraine system (Weidick and Bennike, 2007; Funder *et al.*, 2011). A radiocarbon date from a mollusk fragment retrieved from lake core 13S4-B1 provides additional constraints on moraine deposition before 7970 ± 40 cal a BP. This chronology is consistent with the findings of Young *et al.* (2011a), implicating climate forcing for the deposition of the moraines (Kelly, 1985), rather than ice sheet dynamics controlled by topography and ice-stream dynamics (Warren and Hulton, 1990; Long *et al.*, 2006).

Disko Bugt retreat rates

The deglacial chronologies reconstructed for the Torsukattak (marine-based) and Nordenskiöld (land-based) areas allow us to compare the retreat rates of the two contrasting ice margin settings (Fig. 4). We calculate maximum and minimum possible net retreat rates using the one-sigma ^{10}Be age ranges from our transects (for all information used in calculations see Supplementary Table S1). At Torsukattak fjord, the average ^{10}Be age at sites T1 and T4 are used to obtain a net retreat rate of 45 ± 20 m a⁻¹. We acknowledge that as the elevations

Table 2. Sample information for radiocarbon ages.

Core/site	Latitude (°N)	Longitude (°W)	Lab. no.	Material dated	$\delta^{13}\text{C}$ (‰ PDB)	Age (^{14}C a BP)	Calibrated age (cal a BP $\pm 1\sigma$)	Depth (cm)
Torsukattak fjord 12GRO-Shells-3	69.9793	60.3950	OS-99413	<i>Hiatella arctica</i>	0.03	7930 \pm 40	8260 \pm 60	Surface
Naternaq 13S3-A1 (Lake S3)	68.3031	51.3259	OS-106904	Woody plant remains	-23.24	6580 \pm 35	7470 \pm 40	84.5–86
13S4-B1 (Lake S4)	68.3016	51.3684	OS-107799	Mollusk	0*	7660 \pm 25	7970 \pm 40	99
13CAB-A3 (CAB Lake)	68.4171	50.9341	OS-106903	<i>Daphnia</i> sp., <i>Lepidurus arcticus</i> , <i>Colymbetes dolabratus</i> , <i>Vaccinium uliginosus</i> , <i>Drepanocladus sensu lato</i> sp. remains	-26.16	6250 \pm 35	7200 \pm 30	62–63
13PDY-E3 (Pterodactyl Lake)	68.4130	50.8282	OS-107088	<i>Daphnia</i> sp. and <i>Lepidurus arcticus</i> remains	26*	6270 \pm 35	7210 \pm 40	190.5–191.5
13PDY-A2 (Pterodactyl Lake)	68.4191	50.9163	OS-107094	<i>Drepanocladus sensu lato</i> sp.	-26.77	6330 \pm 35	7250 \pm 70	126–126.5

*Assumed $\delta^{13}\text{C}$ value.

of the ^{10}Be ages vary (102–507 m asl), they are influenced by both thinning and retreat elements of ice margin change. We do not believe this has a major influence on retreat rate calculations that span millennia, and in fact modern observations document that vertical thinning and lateral retreat occur in tandem in similar settings to the north (Kjær *et al.*, 2012). Regardless, unlike the transect at Torsukattak fjord, the transect within the Naternaq study area encompasses the Fjord Stade Moraines. The net rate of retreat over the entire transect (average age of sites N1 and N2 to site N7) is $25 \pm 5 \text{ m a}^{-1}$. The net retreat between the coast (average age of sites N1 and N2) and the Fjord Stade Moraines (site N6) is $40 \pm 10 \text{ m a}^{-1}$. Although both retreat rates calculated for the Nordenskiöld transect are within error of the Torsukattak transect, it may be more reasonable to compare the Torsukattak retreat rate with the coast-site N6 retreat rate from the Nordenskiöld transect, thus not including a stillstand or readvance in either transect.

The similar rates of retreat exhibited by the two sectors of the GrIS before $\sim 9 \text{ ka}$ is striking given the difference in ice margin setting. In marine-based glacier systems, ice dynamics, such as increasing calving rates due to fjord geometry changes, in addition to mass loss to ocean heat transport can play major roles in frontal ablation (Rignot *et al.*, 2010; Carr

et al., 2013; Enderlin *et al.*, 2013). Previous work has documented the ability of marine-based glaciers to rapidly retreat in response to warming during the late Pleistocene (Briner *et al.*, 2009; Hughes *et al.*, 2012; Mangerud *et al.*, 2013), as well as during contemporary periods (Scambos *et al.*, 2004). Our results indicate that when averaged on millennial timescales, land-based glacier systems can retreat as quickly as their marine-based counterparts.

West Greenland retreat rates

We place our results into a wider context by calculating retreat rates for seven additional transects (nine total transects) along the West Greenland coast using previously published ^{10}Be chronologies (Fig. 5; Bennike *et al.*, 2011; Levy *et al.*, 2012; Kelley *et al.*, 2013; Roberts *et al.*, 2013; Young *et al.*, 2013a; Lane *et al.*, 2014; Larsen *et al.*, 2014). Transects for retreat rate calculations were constructed along estimated ice-sheet flow lines, and extend from the present ice margin to the western coastline of Greenland. In all locations where existing chronology allows, a transect mid-point was selected outboard of the Fjord Stade Moraines (using Weidick, 1968), which allows us to compare pre-Fjord Stade Moraine retreat rates. Net retreat rates were calculated for the entire transect

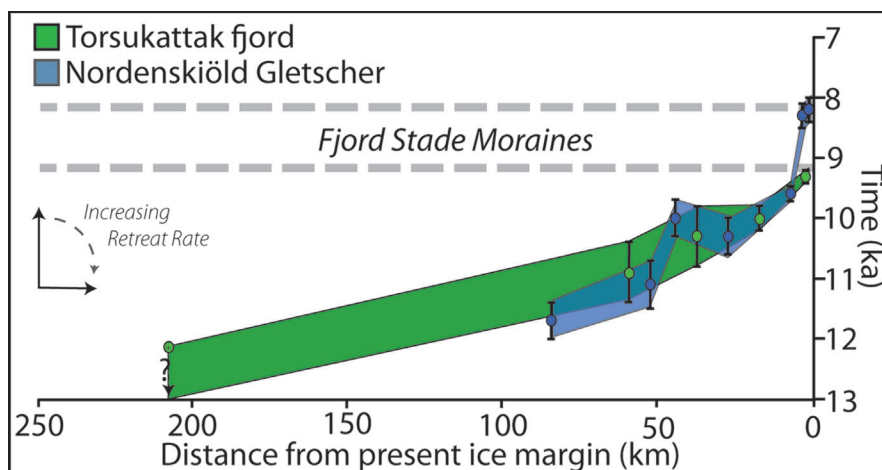


Figure 4. Time–distance diagram of the GrIS margin for four transects in the Disko Bugt region shown in Fig. 1. ^{10}Be age constraints for Torsukattak fjord and Nordenskiöld Gletscher from this study; where multiple ages exist at a single site, the average (\pm one SD) of the ages at a site is used. Note that the outermost site in the Torsukattak transect is a radiocarbon age (from Bennike *et al.*, 1994), and thus is a minimum limiting constraint on deglaciation; all other ages are from ^{10}Be dating. This figure is available in colour online at wileyonlinelibrary.com.

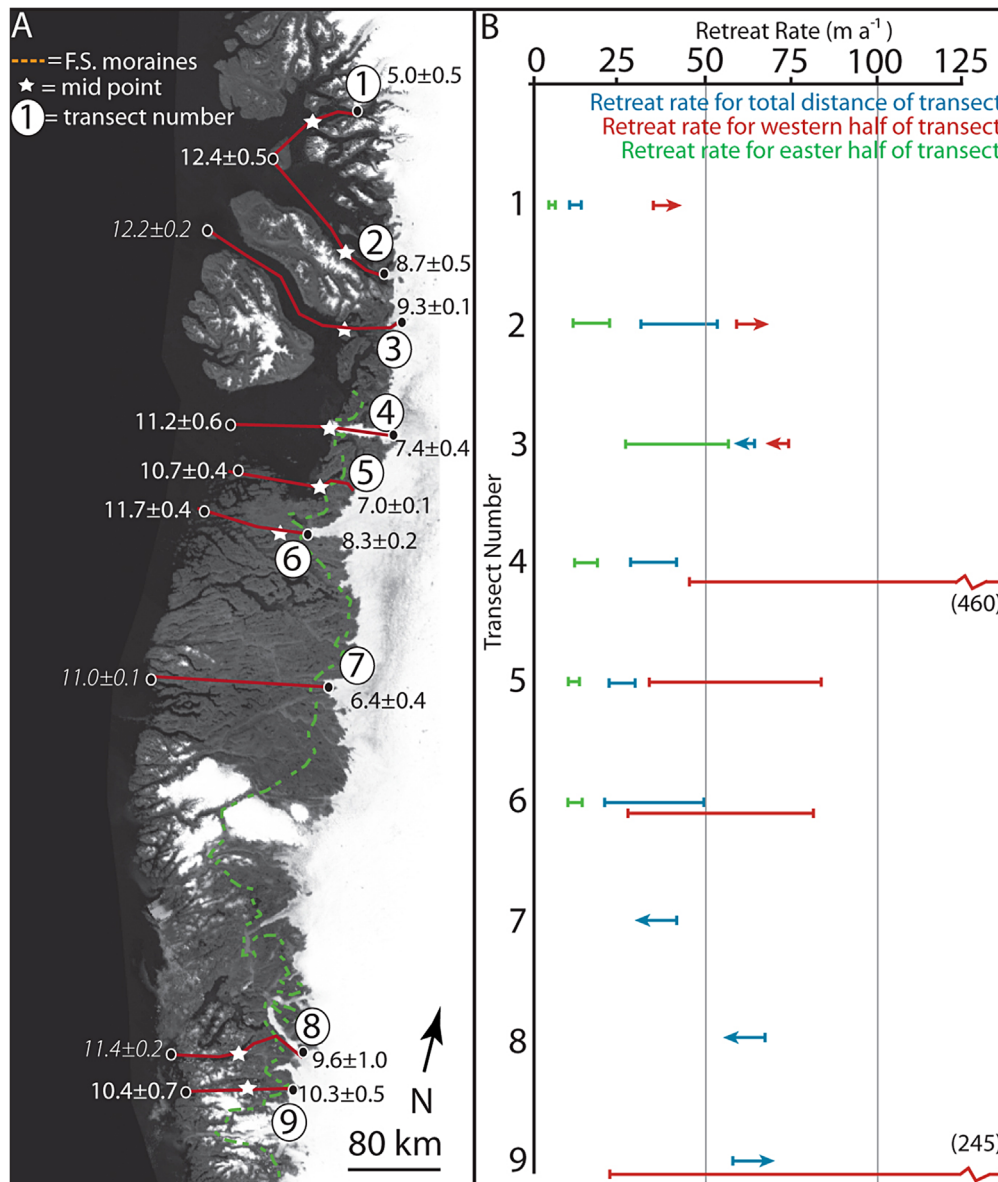


Figure 5. (A) Locations of transects used for calculation of net retreat rates in western Greenland: northern Uummannaq [transect 1; Lane *et al.* (2013); Roberts *et al.* (2013)]; southern Uummannaq [transect 2; Roberts *et al.* (2013)]; Vaigat Strait – Torsukattak fjord [transect 3; this study; Bennike *et al.* (1994)]; central Disko Bugt [transect 4; Kelley *et al.* (2013); Young *et al.* (2013a)]; southern Disko Bugt [transect 5; Kelley *et al.* (2013); Young *et al.* (2013a)]; Nordenskiöld Gletscher system [transect 6; this study]; Sisimiut [transect 7; Bennike *et al.* (2011); Levy *et al.* (2012)]; Godthåbsfjorden [transect 8; Larsen *et al.* (2014)]; Sermilik [transect 9; Larsen *et al.* (2014)]. Overlain on the map are ages (in ka ± 1 SD) for the timing of GrIS retreat onto land and recession east of the present ice margin (radiocarbon ages in italic font, ¹⁰Be ages in plain font). White stars indicate the transect's mid-point (none available for transect 7); orange dotted line denotes the position of the Fjord Stade Moraines from Weidick (1968) and Funder *et al.* (2011). (B) Retreat rate ranges calculated for transects in A. Blue bars indicate net retreat rate for the total transect, red bars denote net retreat rate for the westerly portion of the transect and green bars denote net retreat rate for the easterly portion of the transect. Arrows indicate maximum or minimum retreat rates. For all values used in retreat calculations see Table S1. (For interpretation of the references to color in this figure legend, the reader is referred to the online version of this article.) This figure is available in colour online at wileyonlinelibrary.com.

(from the western coast to the age nearest the present ice margin) for all transects, as well as for a pre-Fjord Stade Moraine subsection for some transects. In some localities where direct ¹⁰Be age control is lacking, minimum-limiting radiocarbon ages were used (transects 3, 7, 8). In these instances only maximum or minimum rates were calculated. Calculations from some transects yielded overlapping ages and therefore infinite retreat rates (transects 1, 2, 7, 8, 9); in these cases only minimum retreat rates are reported.

Two patterns emerge from the comparison of retreat rates along the western GrIS margin. First, net retreat rates for entire transects, which range from 10 to >65 m a⁻¹, are generally similar, and often overlap within error, to those from our two transects near Disko Bugt (25–45 m a⁻¹; Fig. 5).

This similarity exists despite the high degree of variability in the ice margin setting (e.g. marine-based, land-based). For example, retreat rates from fjords such as southern Uummannaq or Torsukattak (eastern portion of transect 3, Fig. 5) are 40 ± 10 and 40 ± 15 m a⁻¹, respectively, while retreat rates from land-based systems such as Nordenskiöld and Sisimiut overlap within error with their marine-based counterparts, with retreat rates of 35 ± 5 and ≤40 m a⁻¹, respectively (Fig. 5). This similarity in retreat rates along the western GrIS margin indicates that on millennial timescales, climate, rather than ice dynamics tied to ice marginal setting, seems to be the dominant factor controlling ice margin fluctuations.

The second pattern revealed through comparison of retreat rates is that retreat rates for the older, westerly portion of the

transects are consistently higher than those calculated for the younger, easterly portion of the transects. In some cases, such as central Disko Bugt, the retreat rate is an order of magnitude higher in the west versus the east. Consistently lower retreat rates in the eastern portion of some transects are due, at least in part, to the fact that the eastern portion of transects encompass the deposition of the Fjord Stade Moraines, as mapped by Weidick (1968). The deposition of the Fjord Stade Moraines throughout West Greenland indicates that even short-lived climate events can elicit a uniform response of the ice sheet.

Farther abroad, retreat rates of $\geq 80 \text{ m a}^{-1}$ (Hughes *et al.*, 2012), $> 58 \text{ m a}^{-1}$ (Briner *et al.*, 2009), $\sim 180 \text{ m a}^{-1}$ (Larter *et al.*, 2014) and $240\text{--}370 \text{ m a}^{-1}$ (Mangerud *et al.*, 2013) have been determined for deglaciation in other marine-based outlet glacier systems. In addition, a detailed study of retreat of numerous marine-based outlet glaciers of the Fennoscandian Ice Sheet reveal retreat rates similar to those in this study, with an average of $\sim 30 \text{ m a}^{-1}$ (Stokes *et al.*, 2014). Land-based ice margin retreat has also been documented, with southern Laurentide Ice Sheet recession estimated to reach as high as 360 m a^{-1} in central North America (Andrews, 1973; Dyke and Prest, 1987), and up to 300 m a^{-1} along the south-eastern Laurentide Ice Sheet (Ridge *et al.*, 2012). These examples document the ability of land-based portions of an ice sheet to retreat on pace with or faster than marine-based parts of ice sheet. This evidence supports our findings from Greenland that on millennial timescales, land-based sectors of ice sheets have the ability to retreat at rates equivalent to marine-based ice sheet sectors.

Ice sheet response time

Collectively, these results from millennial-scale records contrast with what is seen in the historical record, that marine-terminating outlet glaciers retreated more rapidly than land-based ice sheet sectors. Contemporary ice sheet retreat rates vary widely, with a mean glacier retreat recorded in south-east Greenland from AD 1992 to 2000 of 106 m a^{-1} (Moon and Joughin, 2008), although rates $> 1500 \text{ m a}^{-1}$ are calculated for portions of the Pine Island Glacier between AD 1996 and 2009 (Joughin *et al.*, 2010). While contemporary ice sheet retreat rates are variable, the fastest retreating outlet glaciers in West Greenland appear to be dominantly marine-based during the past century (Kelley *et al.*, 2012). The juxtaposition of our millennial-scale records of net ice sheet retreat and more recent retreat rates suggests that time scale is key for understanding the difference between early Holocene retreat rates versus those in historical times, an important point for placing the present observations in context.

We believe that the similarity in retreat rates within our study indicates that climate is the dominant mechanism influencing early Holocene ice margin change. We believe that the ice margin was in equilibrium with climate on millennial or longer timescales due to the relatively synchronous response from the GrIS across such a broad area. However, on shorter timescales, such as the ~ 170 -year historical record of ice margin fluctuation in West Greenland, a strong influence of ice dynamics creates asynchrony in the pattern of GrIS change. This indicates that the response time of the ice margin to changes in climate is variable on the centennial scale and that ice sheet response time to climate is probably < 1000 years for all ice margin types. Brief periods with more rapid retreat may be a feature of our record as well: some segments of our transects demonstrate significantly higher rates on shorter time scales than the net retreat

integrated over multiple millennia. For instance, retreat across central Disko Bugt may have been as high as 450 m a^{-1} during the millennia or less that it took the GrIS to retreat across Disko Bugt. In addition, retreat of marine-based glaciers is well documented for the Fennoscandian Ice Sheet, where net retreat rates are $\sim 30 \text{ m a}^{-1}$ when averaged over multiple millennia, although periods of rapid retreat ($\sim 150 \text{ m a}^{-1}$) occurred on shorter time scales (Stokes *et al.*, 2014).

A large difference between the marine- and land-based glaciers is ice velocity. In a survey of 242 Greenland glaciers, the fastest 140 glaciers are marine-terminating, with marine-terminating glaciers having a peak velocity an order of magnitude higher than land-terminating glaciers (Rignot and Mouginot, 2012). The perturbation theory proposed by Nye (1960) suggests that the local response time of a glacier is the inverse of the local velocity, and thus variability in velocity between ice margin sectors should create varying response times or sensitivity to changes in climatic forcing. Additional factors may enhance the sensitivity of marine-based outlet glaciers to climate change that do not apply to land-based glaciers, such as effects of calving, loss of floating tongues and melting along submarine ice fronts (van der Veen, 2001).

The dichotomy in the behavior of the GrIS outlet glaciers on millennial versus shorter timescales illustrates the varying response time of different glacier systems and the controls velocity may play on different timescales. Asynchronies in the behavior of differing ice margin sectors driven by varying response time of land- versus marine-based ice margins do not appear to be a significant feature in our reconstruction of retreat rates averaged over millennial timescales, while this feature is readily apparent in contemporary records. Therefore, predictions of future ice sheet change must reconcile lags of land-based ice margin sectors on sub-millennial scales, as well as account for the possibility of future retreat of the now stable sections of the ice margin when ice sheet behavior is examined over longer periods.

Conclusions

Our results demonstrate that the GrIS retreated through Torsukattak fjord between ~ 10.9 and $\sim 9.3 \text{ ka}$ at a rate of $45 \pm 20 \text{ m a}^{-1}$. The GrIS retreated from Baffin Bay onto land west of Nordenskiöld Gletscher at $\sim 11.7 \text{ ka}$, with retreat before Fjord Stade moraine deposition occurring at a rate of $40 \pm 10 \text{ m a}^{-1}$. The rate and timing of retreat of the two areas is similar, although the ice margin retreat occurred in a marine setting at one location and in a land-based setting in the other. A compilation of retreat rates from West Greenland demonstrates that net GrIS retreat occurred at rates of about 25 and 45 m a^{-1} , regardless of ice marginal environment. Thus, on millennial timescales, climate rather than dynamics related to ice marginal setting seems to be the dominant control on rate of retreat.

Our finding of synchronous retreat of the GrIS margin on millennial timescales is in contrast to historical observations of faster retreat of marine-terminating outlet glaciers compared with significantly slower retreat of land-based ice margin sectors. This dichotomy in behavior of the ice margin on millennial versus decadal/centennial timescales is probably due to response time of differing ice marginal settings with respect to climatic forcing. Our findings illustrate the ability of land-based sectors of the GrIS margin to retreat at rates comparable to marine-terminating glaciers. We conclude that any significant lag in the response of the GrIS to climate change, past or future, is limited to centennial or shorter timescales.

Supporting information

Additional supporting information may be found in the online version of this article.

Appendix S1. Methodological detail of ^{10}Be dating, radiocarbon sample preparation, and lake coring.

Appendix S2. Lake Physiography and Core Stratigraphy.

Figure S1. Sediment stratigraphy from the five lake cores collected from the Naternaq study area. Table S1. Data used in retreat rate calculations.

Table S1. Data used in retreat rate calculations..

Acknowledgements. We are grateful for laboratory assistance from Sylvia Choi and Matt McClellan, and field assistance from Sandra Cronauer. We thank Nicolaj Larsen and an anonymous reviewer for comments that improved the manuscript. This research was funded by grant NSF-1156361 from the US National Science Foundation Program of Geography and Spatial Science. This is LLNL-JRNL-665782

Abbreviations. GrIS, Greenland Ice Sheet; WGC, West Greenland Current.

References

- Andrews 1973. The Wisconsin Laurentide Ice Sheet: dispersal centers, problems of rates of retreat, and climatic implications. *Arctic and Alpine Research* **5**: 185–199.
- Bennike O, Hansen KB, Knudsen KL *et al.* 1994. Quaternary marine stratigraphy and geochronology in central West Greenland. *Boreas* **23**: 194–215.
- Bennike O, Wagner B, Richter A. 2011. Relative sea level changes during the Holocene in the Sisimiut area, south-western Greenland. *Journal of Quaternary Science* **26**: 353–361.
- Björk AA, Kjær KH, Korsgaard NJ *et al.* 2012. An aerial view of 80 years of climate-related glacier fluctuations in southeast Greenland. *Nature Geoscience* **5**: 427–432.
- Box JE. 2002. Survey of Greenland instrumental temperature records: 1873–2001. *International Journal of Climatology* **22**: 1829–1847.
- Briner JP, Bini AC, Anderson RS. 2009. Rapid early Holocene retreat of a Laurentide outlet glacier through an Arctic fjord. *Nature Geoscience* **2**: 496–499.
- Briner JP, Kaufman DS, Bennike O *et al.* 2014. Amino acid ratios in reworked marine bivalve shells constrain Greenland Ice Sheet history during the Holocene. *Geology* **42**: 75–78.
- Carr JR, Stokes CR, Vieli A. 2013. Recent progress in understanding marine-terminating Arctic outlet glacier response to climatic and oceanic forcing: twenty years of rapid change. *Progress in Physical Geography* **37**: 436–467.
- Donner J, Jungner H. 1975. Radiocarbon dating of shells from marine Holocene deposits in the Disko Bugt area, West Greenland. *Boreas* **4**: 25–45.
- Dyke AS, Prest VK. 1987. Late Wisconsinan and Holocene History of the Laurentide Ice Sheet. *Geographie Physique et Quaternaire* **41**: 237–263.
- Dyke LM, Hughes ALC, Murray T *et al.* 2014. Evidence for the asynchronous retreat of large outlet glaciers in southeast Greenland at the end of the last glaciation. *Quaternary Science Reviews* **99**: 244–259.
- Enderlin EM, Howat IM, Vieli A. 2013. High sensitivity of tidewater outlet glacier dynamics to shape. *Cryosphere Discussions* **7**: 551–572.
- Frich P, Ingólfsson O. 1990. Det holocæne sedimentationsmiljø ved Igpiik samt en model for den relative landhævning i Disko Bugt området, Vestgrønland. *AËrsskrift for Dansk Geologisk Forening* **1987** **89**: 1–10.
- Funder S, Kjeldsen KK, Kjær KH *et al.* 2011. The Greenland Ice Sheet during the past 300, 000 years: a review. In Elhers J, Gibbard PL (eds). *Quaternary glaciations—extent and chronology*. Elsevier Science: Amsterdam **15**: 699–713.
- Hogan KA, Dowdeswell JA, Ó Cofaigh C *et al.* 2012. Glacimarine sedimentary processes and depositional environments in an embayment fed by West Greenland ice streams. *Marine Geology* **311–314**: 1–16.
- Holland DM, Thomas RH, De Young B *et al.* 2008. Acceleration of Jakobshavn Isbræ triggered by warm subsurface ocean waters. *Nature Geoscience* **1**: 659–664.
- Hughes ALC, Rainsley E, Murray T *et al.* 2012. Rapid response of Helheim Glacier, southeast Greenland, to early Holocene climate warming. *Geology* **40**: 427–430.
- Ingólfsson Ó, Frich P, Funder S *et al.* 1990. Paleoclimatic implications of an early Holocene glacier advance on Disko island, West Greenland. *Boreas* **19**: 297–311.
- Jennings AE, Walton ME, Ó Cofaigh C *et al.* 2014. Paleoenvironments during Younger Dryas-Early Holocene retreat of the Greenland ice sheet from outer Disko trough, central west Greenland. *Journal of Quaternary Science* **29**: 27–40.
- Joughin I, Smith BE, Holland DM. 2010. Sensitivity of 21st century sea level to ocean-induced thinning of Pine Island Glacier, Antarctica. *Geophysical Research Letters* **37**: L200502.
- Kelley SE, Briner JP, Young NE *et al.* 2012. Maximum Late Holocene extent of the western Greenland Ice Sheet during the late 20th century. *Quaternary Science Reviews* **56**: 89–98.
- Kelley SE, Briner JP, Young NE. 2013. Rapid ice retreat in Disko Bugt supported by ^{10}Be dating of the last recession of the western Greenland Ice Sheet. *Quaternary Science Reviews* **82**: 13–22.
- Kelly M. 1985. A review of the Quaternary geology of western Greenland. In *Quaternary Environments; Eastern Canadian Arctic, Baffin Bay and Western Greenland*, Andrews JT (ed.). London: Allen & Unwin. pp. 461–501.
- Khan SA, Kjær KH, Bevis M *et al.* 2014. Sustained mass loss of the northeast Greenland ice sheet triggered by regional warming. *Nature Climate Change* **4**: 292–299.
- Kjær KH, Khan SA, Korsgaard NJ *et al.* 2012. Aerial photographs reveal late-20th-century dynamic ice loss in northwestern Greenland. *Science* **337**: 569–573.
- Lal D. 1991. Cosmic ray labeling of erosion surfaces: in situ nuclide production rates and erosion models. *Earth and Planetary Science Letters* **104**: 424–439.
- Lane TP, Roberts DH, Rea BR *et al.* 2014. Controls upon the Last Glacial Maximum deglaciation of the northern Uummannaq Ice Stream System, West Greenland. *Quaternary Science Reviews* **92**: 324–344.
- Larsen NK, Funder S, Kjær KH *et al.* 2014. Rapid early Holocene ice retreat in West Greenland. *Quaternary Science Reviews* **92**: 310–323.
- Larter RD, Anderson JB, Graham AGC *et al.* 2014. Reconstruction of changes in the Amundsen Sea and Bellingshausen Sea sector of the West Antarctic Ice Sheet since the Last Glacial Maximum. *Quaternary Science Reviews* **100**: 55–86.
- Levy LB, Kelly MA, Howley JA *et al.* 2012. Age of the Ørkendalen moraines, Kangerlussuaq, Greenland: constraints on the extent of the southwestern margin of the Greenland Ice Sheet during the Holocene. *Quaternary Science Reviews* **52**: 1–5.
- Lloyd J, Moros M, Perner K *et al.* 2011. A 100 yr record of ocean temperature control on the stability of Jakobshavn Isbræ, West Greenland. *Geology* **39**: 867–870.
- Lloyd J, Park L, Kuijpers A *et al.* 2005. Early Holocene palaeoceanography and deglacial chronology of Disko Bugt, west Greenland. *Quaternary Science Reviews* **24**: 1741–1755.
- Long AJ, Roberts DH. 2002. A revised chronology for the 'Fjord Stade' moraine in Disko Bugt, west Greenland. *Journal of Quaternary Science* **17**: 561–579.
- Long AJ, Woodroffe SA, Roberts DH *et al.* 2011. Isolation basins, sea-level changes and the Holocene history of the Greenland Ice Sheet. *Quaternary Science Reviews* **30**: 3748–3768.
- Long AJ, Roberts DH, Dawson S. 2006. Early Holocene history of the west Greenland Ice Sheet and the GH-8.2 event. *Quaternary Science Reviews* **25**: 904–922.
- Long AJ, Roberts DH, Rasch M. 2003. New observations on the relative sea level and deglacial history of Greenland from Innaarsuit, Disko Bugt. *Quaternary Research* **60**: 162–171.
- Long AJ, Roberts DH, Wright MR. 1999. Isolation basin stratigraphy and Holocene relative sea-level change on Arveprinsen Ejlund,

- Disko Bugt, West Greenland. *Journal of Quaternary Science* **14**: 323–345.
- Mangerud J, Goehring BM, Lohne ØS *et al.* 2013. Collapse of marine-based outlet glaciers from the Scandinavian Ice Sheet. *Quaternary Science Reviews* **67**: 8–16.
- Möller P, Larsen NK, Kjær KH *et al.* 2010. Early to middle Holocene valley glaciations on northernmost Greenland. *Quaternary Science Reviews* **29**: 3379–3398.
- Moon T, Joughin I. 2008. Changes in ice front position on Greenland's outlet glaciers from 1992 to 2007. *Journal of Geophysical Research* **113**: n F2.
- Nye JF. 1960. The response of glaciers and ice-sheets to seasonal and climatic changes. Proceedings of the Royal Society of London. *Series A. Mathematical and Physical Sciences* **256**: 559–584.
- O Cofaigh C, Dowdeswell JA, Jennings AE *et al.* 2013. An extensive and dynamic ice sheet on the West Greenland shelf during the last glacial cycle. *Geology* **41**: 219–222.
- Quillmann U, Andrews JT, Jennings AE. 2009. Radiocarbon dates from marine sediment cores of the Iceland, Greenland, and northeast Canadian Arctic shelves and Nares Strait. *Institute of Arctic and Alpine Research Occasional Paper* **59**: 14–15.
- Ridge JC, Balco G, Bayless RL *et al.* 2012. The new North American varve chronology: A precise record of southeastern Laurentide Ice Sheet deglaciation and climate, 18. 2–12. 5 kyr BP, and correlations with Greenland ice core records. *American Journal of Science* **312**: 685–722.
- Rignot E, Koppes M, Velicogna I. 2010. Rapid submarine melting of the calving faces of West Greenland glaciers. *Nature Geoscience* **3**: 187–191.
- Rignot E, Mouginot J. 2012. Ice flow in Greenland for the international polar year 2008–2009. *Geophysical Research Letters* **39**: doi: 10.1029/2012GL051634.
- Rinterknecht V, Jomelli V, Brunstein D *et al.* 2014. Unstable ice stream in Greenland during the Younger Dryas cold event. *Geology* **42**: 759–762.
- Roberts DH, Rea BR, Lane TP *et al.* 2013. New constraints on Greenland ice sheet dynamics during the last glacial cycle: evidence from the Uummannaq ice stream system. *Journal of Geophysical Research: Earth Surface* **118**: 519–541.
- Scambos TA, Bohlander J, Shuman C *et al.* 2004. Glacier acceleration and thinning after ice shelf collapse in the Larsen B embayment, Antarctica. *Geophysical Research Letters* **31**: L18402.
- Seidenkrantz M.-S, Roncaglia L, Fischel A *et al.* 2008. Variable North Atlantic climate seesaw patterns documented by a late Holocene marine record from Disko Bugt, West Greenland. *Marine Micropaleontology* **68**: 66–83.
- Stokes CR, Corner GD, Winsborrow MCM. *et al.* 2014. Asynchronous response of marine-terminating outlet glaciers during deglaciation of the Fennoscandian Ice Sheet. *Geology* **42**: 455–458.
- Stone JO. 2000. Air pressure and cosmogenic isotope production. *Journal of Geophysical Research* **105**: 23753–23759.
- Tauber H. 1960. Copenhagen radiocarbon dates IV. *American Journal of Science: Radiocarbon Supplement* **6**: 215–225.
- van der Veen CJ. 2001. Greenland ice sheet response to external forcing. *Journal of Geophysical Research: Atmospheres* **106**: 34047–34058.
- Vinther BM, Buchardt SL, Clausen HB. *et al.* 2009. Holocene thinning of the Greenland ice sheet. *Nature* **461**: 385–388.
- Warren C, Hulton N. 1990. Topographic and glaciological controls on Holocene ice-sheet margin dynamics, central West Greenland. *Annals of Glaciology* **14**: 307–310.
- Weidick A. 1968. Observations on some Holocene glacier fluctuations in west Greenland. *Meddeleser om Grønland* **165**: 202.
- Weidick A. 1974. *Quaternary map of Greenland, 1 : 500,000 Sheet 3, Søndre Strømfjord-NÛgssuaq Kvartergeologisk*. Copenhagen: Greenland Geologic Survey.
- Weidick A. 1994. Historical fluctuations of calving glaciers in south and West Greenland. *Rapport Grønlands Geologiske Undersøgelse* **161**: 73–79.
- Weidick A, Bennike O. 2007. Quaternary glaciation history and glaciology of Jakobshavn Isbræ and the Disko Bugt region, West Greenland: a review. Copenhagen: Geological Survey of Denmark and Greenland.
- Weidick A, Bennike O, Citterio M. *et al.* 2012. Neoglacial and historical glacier changes around Kangersuneq fjord in southern West Greenland. *Copenhagen: Geological Survey of Denmark and Greenland*.
- Young NE, Briner JP, Axford Y *et al.* 2011a. Response of a marine-terminating Greenland outlet glacier to abrupt cooling 8200 and 9300 years ago. *Geophysical Research Letters* **38**: L24701.
- Young NE, Briner JP, Rood DH *et al.* 2013a. Age of the Fjord Stade moraines in the Disko Bugt region, western Greenland, and the 9.3 and 8.2 ka cooling events. *Quaternary Science Reviews* **60**: 76–90.
- Young NE, Briner JP, Stewart HAM. *et al.* 2011b. Response of Jakobshavn Isbræ, Greenland, to Holocene climate change. *Geology* **39**: 131–134.
- Young NE, Schaefer JM, Briner JP *et al.* 2013b. A ¹⁰Be production-rate calibration for the Arctic. *Journal of Quaternary Science* **28**: 515–526.
- Zwally HJ, Abdalati W, Herring T. *et al.* 2002. Surface melt-induced acceleration of Greenland ice-sheet flow. *Science* **297**: 218–222.